Sādhanā, Vol. 26, Parts 1 & 2, February–April 2001, pp. 179–198. © Printed in India

Solidification control in continuous casting of steel

S MAZUMDAR and S K RAY

R&D Centre for Iron and Steel, Steel Authority of India Ltd (SAIL), Ranchi, India
e-mail: maz@rdcis.bih.nic.in

Abstract. An integrated understanding of heat transfer during solidification, friction/lubrication at solid–liquid interface, high temperature properties of the solidifying shell etc. is necessary to control the continuous casting process. The present paper elaborates upon the knowledge developed in the areas of initial shell formation, mode of mould oscillation, and lubrication mechanism. The effect of these issues on the caster productivity and the quality of the product has been discussed. The influence of steel chemistry on solidification dynamics, particularly with respect to mode of solidification and its consequence on strength and ductility of the solidifying shell, has been dealt with in detail. The application of these basic principles for casting of stainless steel slabs and processing to obtain good quality products have been covered.

Keywords. Continuous casting; early solidification; mould oscillation; lubrication; mode of solidification; strength and ductility of shell; microsegregation.

1. Introduction

Solidification in continuous casting (CC) technology is initiated in a water-cooled open-ended copper mould. The steel shell which forms in the mould contains a core of liquid steel which gradually solidifies as the strand moves through the caster guided by a large number of roll pairs. The solidification process initiated at meniscus level in the mould is completed in secondary cooling zones using a combination of water spray and radiation cooling.

Solidification speciality of CC technology arises from the dynamic nature of the casting process. In particular this relates to

- handling of very high heat flux in the mould,
- nurturing of the initial thin and fragile solid shell for avoidance of breakout during descent of the strand down the mould,
- designing of casting parameters in tune with the solidification dynamics of the steel grade for minimisation or elimination of surface and internal defects in the cast product.

Safe caster operation (i.e. without metal breakout) and achievement of acceptable product quality, require understanding of both process engineering and metallurgy of solidification. The present review deals with core concepts in regard to friction control in the mould and the impact of grade characteristics on the solidification process. The former is a unique example of combination of solidification mechanism and process engineering, and the latter defines the casting parameters to be applied to casting of diverse steel grades.

2. Initial shell formation and oscillation effect

Early solidification in continuous casting occurs in the form of partial freezing of the meniscus curvature originating from the mould liquid contact point. Prevention of sticking and tearing of this initial thin shell during the descent of the solidifying strand is one of the major functions of the CC mould. To minimise shell sticking and tearing, friction between the strand surface and mould wall must be kept below a critical level depending upon the shell strength. Minimisation of the friction and continuous release of the shell from the mould have been achieved through the introduction of mould oscillation aided by lubrication. A historical overview of this key engineering innovation, which enables commercial application of continuous casting has been recently published (Szekeres 1996).

The main features of the oscillation cycle prevalent now is depicted in figure 1a. The figure represents the evolution of the mould velocity in one cycle under the sinusoidal mode. The oscillation cycle influences mould-strand friction including release of the strand from the mould and also defines surface topography of the cast product. From the lubrication point of view, the oscillation cycle translates into two operating phases as below.

(1) A compression phase of duration t_N defined as the negative strip time where mould slag is infiltrated into the gap between the first solidified shell and the mould. The period t_N witnesses a higher downward velocity of the mould relative to descending velocity of the strand (Vc) and is responsible for the release of the shell from the mould wall.
(2) A lubrication phase of duration t_P where tensile stresses are applied to the first solidified shell accompanied by deposition of the infiltrated mould slag against the mould wall. This corresponds to upward movement of the mould.

Effect of oscillation in terms of friction pattern during upward and downward stroke is shown in figure 1b (Brendzy *et al* 1993). The measured load cell response indicates the friction pattern under sinusoidal oscillation, i.e. high friction during upstroke and minimal friction centred about the negative strip time. Loss of friction during t_N suggests decoupling of the shell from the mould wall. Figures 1c & d (Takeuchi *et al* 1991) also show results of various other changes caused by oscillation, e.g. mould slag pressure and inflow rate of slag.

Mould oscillation results in formation of oscillation marks (OM) at near regular intervals on the surface of the cast product. These marks may be accompanied by

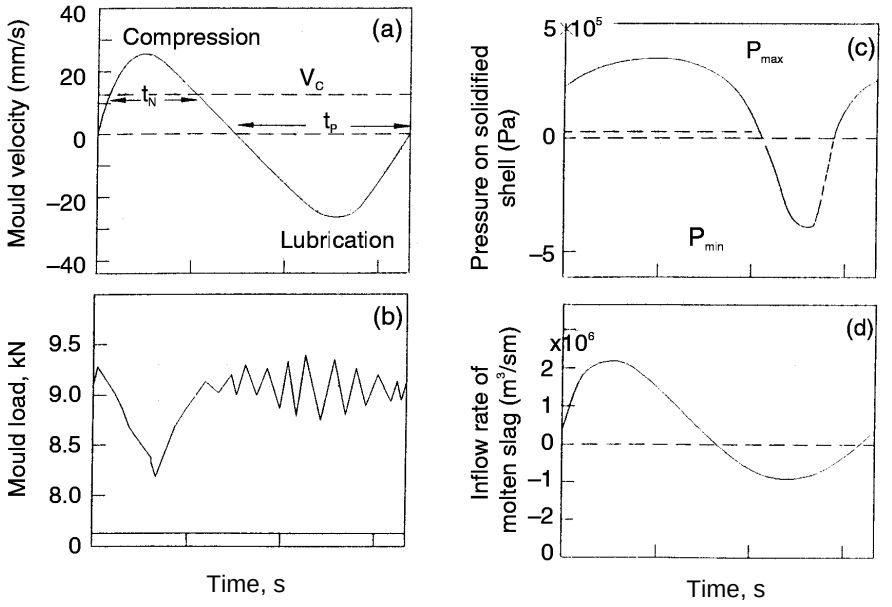

Figure 1. Effect of mould oscillation on (**a**) negative and positive strip time (t_n, t_p), (**b**) mould load representing friction (Brendzy *et al* 1993), (**c**) slag pressure on solidified shell (Takeuchi *et al* 1991), and (**b**) inflow rate of molten slag (Takeuchi *et al* 1991).

formation of solidified hooks beneath the oscillation marks as shown in figure 2. Formation of oscillation marks basically comprises three main stages.

- Partial solidification of the meniscus against the mould wall and the mould powder in the form of a fragile hook.
- Bending of the hook during t_N and healing of any shell tear (caused by viscous drag in the preceding upstroke). The segregation line shown in figure 2 is attributed to shell bending, where the solute-rich interdendritic liquid is squeezed out to the surface (Harada *et al* 1990). The origin of shell bending in slab casting is variously traced to:

  – Collision of slag rim with top of the solid shell (Tada *et al* 1984).
  – Pressure of infiltrating molten mould slag (Takeuchi & Brimacombe1984).

- Shell unbending during upstroke by viscous drag (Wolf 1991a). The upstroke may also be associated with overflow of liquid metal over the bent hook in case of strong meniscus shell or mould level rise. A combination of shell unbending and metal overflow is also possible (Saucedo 1991). The oscillation marks tend to be deeper in case of shell unbending, while these are shallow and show lapped surfaces when overflow occurs.

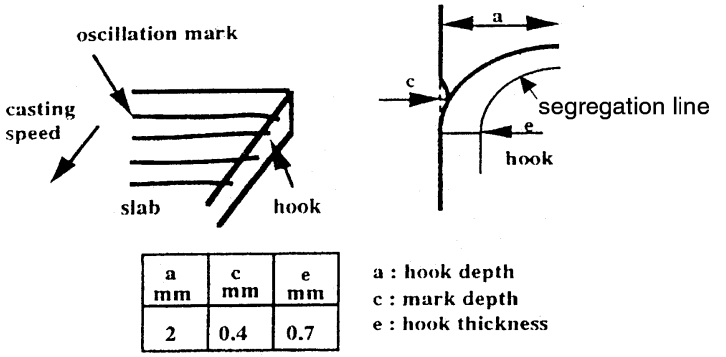

a mm	c mm	e mm
2	0.4	0.7

Figure 2. Oscillation mark and solidification hook with indicative dimensions.

Various types of oscillation marks and hooks encountered in slab casting as mentioned above are shown in figure 3. It is evident from the figure that the shape of hook and oscillation marks is basically linked to the extent of shell bending/unbending and overflow over the meniscus during casting.

2.1 *Lubrication mechanism in the mould*

Lubrication in the slab mould arises from the infiltration of mould slag into the strand mould gap. The layering of the slag in the gap is shown in figure 4. The friction in the mould is considered to originate from two mechanisms. The motion of the mould relative to the solidified shell gives rise to a frictional force due to the viscosity of the slag film. The frictional force generated through this mechanism, termed liquid friction f_l is given by

$$f_l = h(Vm - Vc)/d_l \tag{1}$$

where, Vm = mould speed, Vc = casting speed, h = viscosity of liquid slag film, and d_l = thickness of slag film.

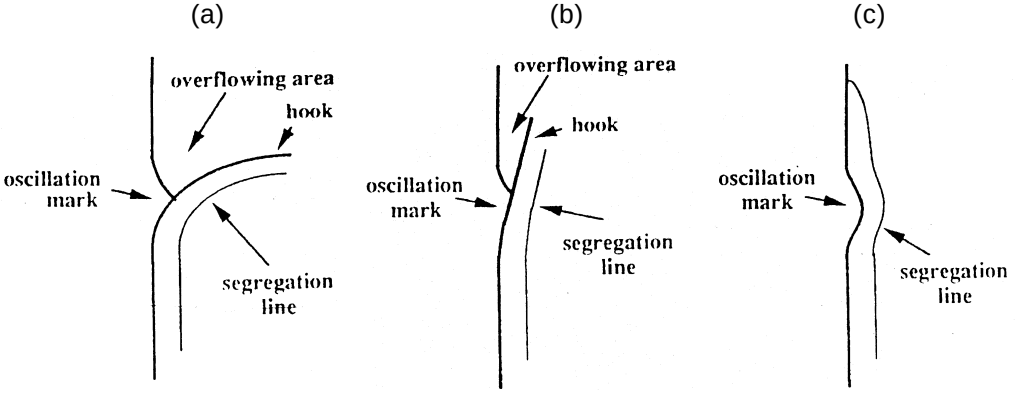

Figure 3. Types of oscillation marks and hooks in slab casting: (**a**) hook reciprocating the meniscus shape, (**b**) straight hook, and (**c**) bent or folding hook.

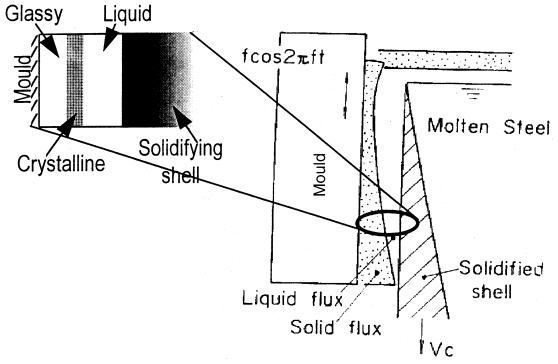

Figure 4. Schematic view of mould slag between mould wall and solidified shell.

If relative movement occurs between the strand and the solidified mould slag, the friction force is generated by solid–solid contact. The resulting solid friction f_s is expressed as

$$f_s = h_s H \tag{2}$$

where h_s = coefficient of solid friction, and H = ferrostatic pressure of molten steel.

The relative influence of f_l and f_s along the mould length is shown in figure 5 (Suzuki *et al* 1991). The figure shows that liquid lubrication (f_l) dominates completely in the upper part of the mould. On the other hand, the value of the solid friction f_s is lower than f_l at the lower part of the mould indicating dominance of solid lubrication. The figure also brings out the role of slag viscosity in determining the zone of influence of f_l. With lower slag viscosity the zone of liquid lubrication extends further into the lower part of the mould.

The friction concept as mentioned above is useful in explaining the increased tendency of sticker breakout with increase in casting speed. A comparison between calculated tensile stress on the solidified shell and high temperature strength of 0.1% C steel is made in figure 6. The tensile stress, s_f, applied to the solidified shell at location, Z, from the meniscus is calculated using (Suzuki *et al* 1991).

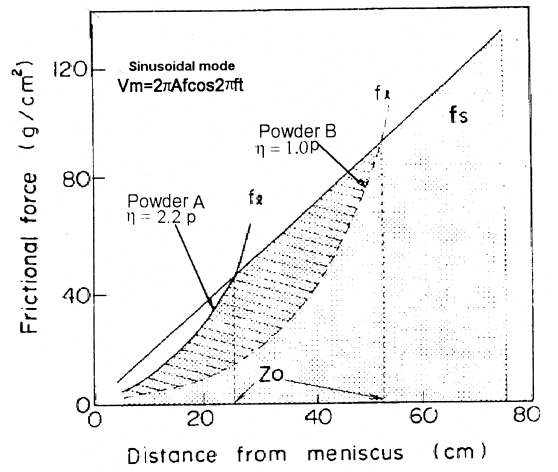

Figure 5. Zones of liquid friction (f_l) and solid friction (f_s) control in C.C. mould (Suzuki *et al* 1991).

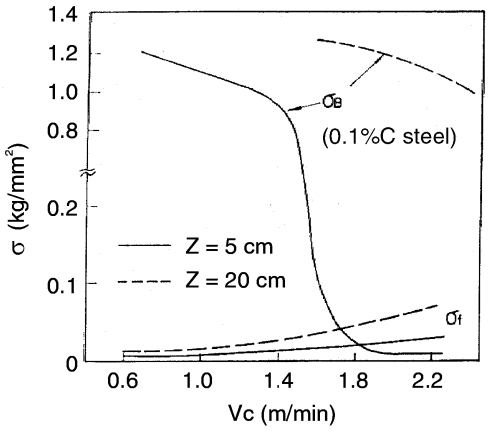

Figure 6. Comparison between tensile stress on solidified shell and high temperature strength of steel (Suzuki *et al* 1991).

$$s_f = \int_0^z F\mathrm{d}z / D_s, \tag{3}$$

where F = frictional force (f_l or f_s) per unit area whichever is lower, and D_s = thickness of solidified shell at Z.

Figure 6 shows that s_f exceeds shell strength s_b at 5 cm from the meniscus with a casting speed of 1·8 m/min, indicating that sticking type breakout may occur.

Friction analysis indicates that prevention of sticking type breakout in high speed casting requires improvement in the lubrication in the upper part of the mould, particularly just below the meniscus. Since liquid lubrication completely prevails near the meniscus, the optimum casting conditions can be ascertained using (1). As the equation indicates, this calls for consideration of mould slag properties (viscosity and solidification temperature), as well as the oscillation parameters.

2.2 *Mode of oscillation*

The analysis in the previous sections indicated the important role of oscillation parameters, e.g. negative strip time (t_N) and mould up time (t_P) on initial shell formation and friction control. These parameters, under more common sinusoidal mode of oscillation, are defined by.

$$t_N = (1/pf)\cos^{-1}(V_o/phf),$$
$$t_P = \tfrac{1}{2}\, t_0. \tag{4}$$

The expressions for t_N, t_P show that the sinusoidal mode is characterized by only two independent parameters such as stroke and frequency. These two degrees of freedom are not sufficient to optimise independently the duration of t_N and t_P.

In order to separate the lubrication function and the compression on the solidified shell, the triangular mode of oscillation is steadily gaining ground (Darle *et al* 1993). The triangular mode permits control of a third parameter, i.e. triangle distortion, a defined as,

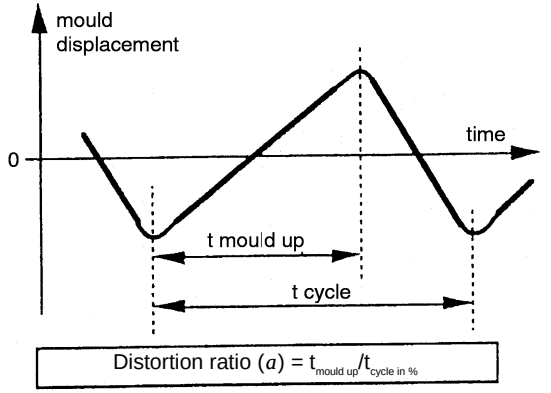

Figure 7. Triangular mode of oscillation (Darle *et al* 1993).

$$a(\%) = (t_P/t_C) \times 100. \quad (5)$$

The features of this oscillation mode are shown in figure 7 indicating longer upward motion as compared to downward motion. The duration of up motion (i.e. t_P) can be regulated as per requirement by adjusting distortion ratio (a). Consequent to longer t_P, the relative speed of the mould to the solidifying shell decreases resulting in reduced friction. Comparison of measured mould friction between sinusoidal and non sinusoidal mode on a pilot caster is shown in figure 8 (Wolf 1991a).

Finally it may be added that the concept of non-sinusoidal motion, though known for long, is only now finding application in commercial slab casting with development of the hydraulic oscillation mechanism (Hoedle *et al* 1999).

2.3 *Early solidification performance*

The performance of the oscillation and lubrication process in slab casting is primarily indicated by oscillation mark depth, hook depth and powder consumption. Salient features of these indicators are discussed below.

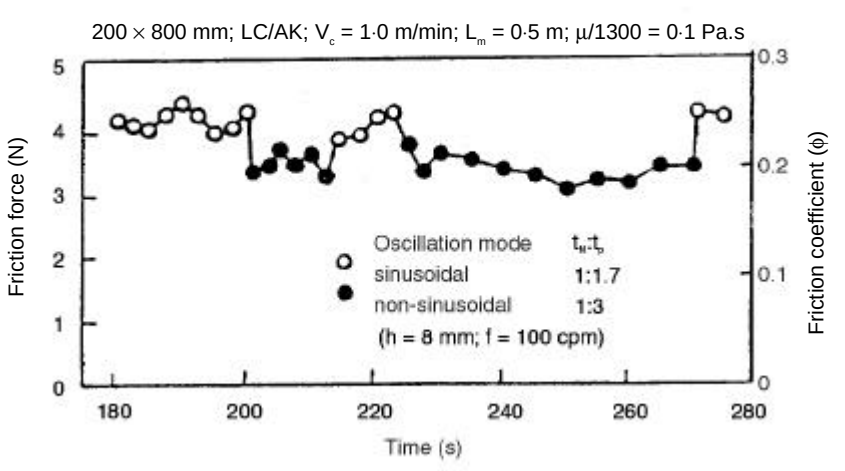

Figure 8. Comparison of mould friction for sinusoidal and triangular oscillation (Wolf 1991).

2.3*a* *Oscillation mark depth:* This mark in itself is a surface defect and its severity may prevent hot rolling without prior grinding in special grades such as austenitic stainless steel. Increased thermal resistance at the bottom of mark reduces local cooling rate which retards shell growth and coarsens local microstructure. Such coarse microstructure enhances susceptibility for transverse surface/subsurface cracks, particularly in peritectic steel grades (Wolf 1991b).

The most critical factor controlling mark depth is steel composition. The strong meniscus shell of peritectic steel grades (about 0·1% C) and austenitic stainless steel (Ni/Cr ratio = 0·55) leads to most pronounced mark formation. In higher carbon steels with weak meniscus shells, on account of enhanced microsegregation, oscillation marks are much less severe. The composition dependence of mark depth is rationalised in figure 9 (Wolf 1991b), where the effect of the carbon percentage on phosphorus segregation and mark depth are shown.

The other factors associated with oscillation mark formations relate to the mechanism of shell bending and unbending mentioned earlier. Mark depth is enhanced due to the inward bending of the meniscus shell during the down-stroke due to the flux pressure of the liquid slag. Calculated flux pressure distribution during the down-stroke showed that down-bending during the whole period of negative strip is decisive, while the instance of maximum velocity is not. In practical terms, mark depth can thus

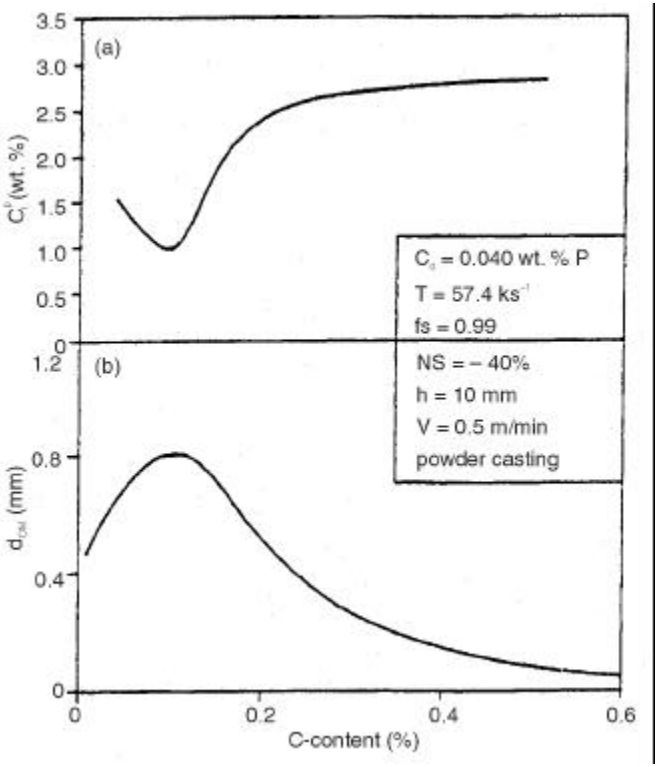

Figure 9. Effect of carbon content on (**a**) phosphorus segregation in meniscus shell, C_l^p, and (**b**) oscillation mark depth d_{OM} (Wolf 1991a).

be correlated to t_N and powder consumption. Higher consumption causes deeper marks on account of larger flux volume driven during down-stroke.

2.3*b* *Hook depth*: As compared to oscillation marks, hooks (figure 3) are more subtle defects, and largely affect subsurface cleanliness of low to ultra low carbon steel slabs. The effect of the hook shows up in the form of slivers in the vicinity of coil edges (rolled slab) corresponding to slab corners. For very low carbon grades (%C ≤ 0·01%), the slivers may appear in the centre of the coil width as well (Darle *et al* 1993).

The geometry of the solidified hooks vary according to casting conditions as explained in figure 3. Hooks reciprocating the meniscus shape (figure 3a) and to a lesser extent, straight hooks (figure 3b), act as carriers of mould slag into the slab subsurface (up to about 2 mm). Subsequent metal overflow embeds these in the solidified shell. In the case of bent or folding hooks, on the other hand, slag adhering to the meniscus shell returns to the surface and does not undermine slab cleanliness. Hook formation is highly sensitive to carbon content of steel on account of low liquidus–solidus gap, and predominantly occurs in corner regions of slabs which encounter stronger mould cooling. In the case of ultra-low carbon grades, hooks appear in the slab midface regions also (Darle *et al* 1993).

The hook defect which arises from overflow of the meniscus shell requires close control of metal level in the mould. Oscillation parameters also influence hook depth. Non-sinusoidal oscillation is shown to be an effective tool for improving slab subsurface cleanliness. The combination of lower inward bend (low t_N) and higher outward bend (high t_P) accompanying high triangular distortion provides additional means to control hook geometry.

2.3*c* *Powder consumption*: A practical indicator of mould friction is consumption rate of powder. It is apparent that powder consumption is proportional to the total fraction of the liquid and solid slag layer which is sheared off and carried away by the strand surface and must be replenished by powder feeding. Very low consumption indicates less liquid film and hence high friction. It may be worthwhile to note that for stable lubrication in slab casting, powder consumption of around 0·3 kg/m^2 is an often assumed target value (Andrezejewski *et al* 1990).

Quantitative assessment of the powder consumption, however, still eludes theoretical modelling. Nevertheless, several empirical formulations have been proposed (Wolf 1991). These formulations relate powder consumption (Q_r, kg/m^2) to oscillation and mould slag parameters.

$$Q_r = 0{\cdot}55\ t_c(mV_c^2)^{-0{\cdot}5} + 0{\cdot}1, \tag{6}$$

where m = slag viscosity at 1300°C, and t_c = total cycle time.

Comparison of measured powder consumption for low carbon slab casting, and that using (6) is made in figure 10. The prediction, though reasonably good, somewhat underestimates the measured values at high frequency. The formulation brings out decrease of consumption with an increase in either slag viscosity, casting speed or oscillation frequency. However, it does not take into account either steel solidus

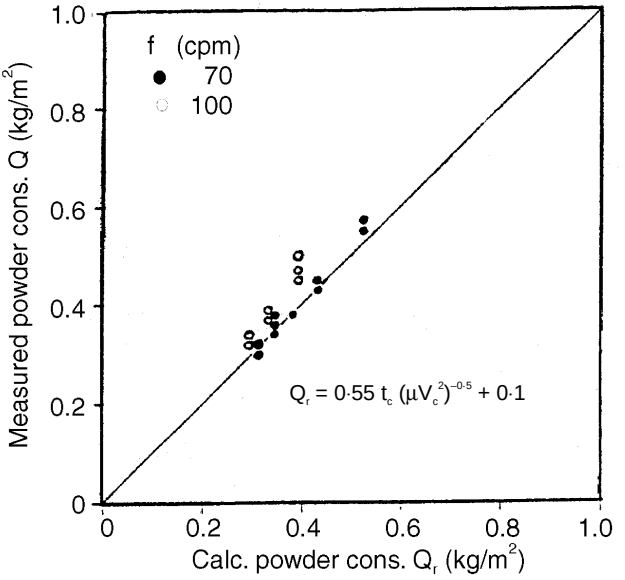

Figure 10. Comparison of measured and calculated powder consumption (Wolf 1991a).

temperature or solidification temperature of the molten slag which controls the extent of liquid slag film along the strand surface in the mould.

2.3*d* *Control guideline*: Analyses of factors associated with oscillation mark depth, hook depth and powder consumption (i.e. friction control) show considerable contradictions, i.e. all performance requirements cannot be met simultaneously. Most significant of these are:

- Oscillation parameters responsible for reduced mark depth (i.e. short stroke and high frequency) contribute to rise in mould friction.
- Enhanced powder consumption required for reduction of friction necessitates low mould slag viscosity. But low slag viscosity is detrimental to slag film stability under ferrostatic pressure. Thus conventional optimisation practice prefers to use higher slag viscosity for friction control.

It is, therefore, necessary to adjust the casting parameters in accordance with the problems to be remedied. In the case of sinusoidal oscillation, this implies using long stroke/low frequency for sticker grades (for minimum friction), and short stroke/high frequency for depression grades (for mark depth control). In the case of triangular oscillation, the required changes can be achieved through control of distortion ratio (a). Similarly, to compensate for friction increase due to higher slag viscosity, reduction in solidification temperature of the slag is an option well-suited to sticker grades.

3. Influence of steel grades on solidification dynamics

Surface and subsurface quality of continuously cast product is largely influenced by solidification conditions inside the mould (Brimacombe 1993). Internal quality is additionally affected by bulging of the solidifying strand below the mould. For a specific caster configuration and machine condition, steel chemistry plays an important role in controlling the solidification characteristics. Solidification structure, microsegregation, and the high-temperature strength & ductility are predominantly decided by the relative proportions of *d* (ferrite) and *g* (austenite) formed during and subsequent to solidification.

3.1 *Solidification mode*

The high-temperature region of the Fe–C equilibrium phase diagram is shown in figure 11. The proportions of *d* and *g* forms in the solid fraction at the peritectic

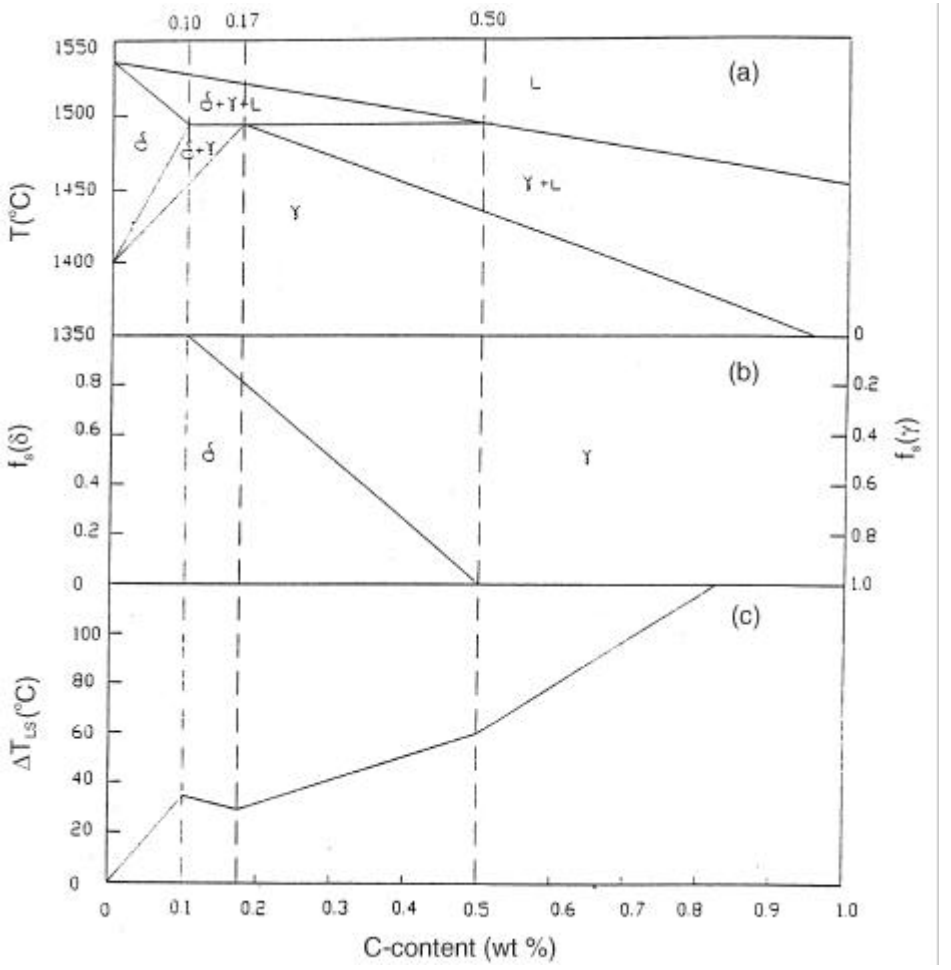

Figure 11. Influence of carbon content on extent of *d–g* phase.

temperature, and the temperature interval between equilibrium solidus and liquidus, are also indicated in the figure. Up to 0·1% carbon, solidification takes place completely through the *d* mode. The mode is fully *g* above 0·5%, and is mixed in the intermediate carbon range. The relative proportion of *d* and *g* forms in the solidified shell can be defined on the basis of 'ferrite potential' (FP) expressed as (Wolf 1991)

$$FP = 2{\cdot}5(0{\cdot}5 - \%C). \tag{7}$$

FP above 1 is indicative of ferritic mode of solidification. Negative value corresponds to fully austenitic solidification, and FP between 0 and 1 indicates mixed mode. Stainless steel encompasses a wide chemistry range with many alloying elements. Unlike for plain carbon steel, the Fe–C phase diagram is not indicative of the proportion of *d* and *g* formed during and subsequent to solidification of stainless steel. Ni and Cr being the two common alloying elements, respectively *g* and *d* stabilisers, the other elements are expressed as equivalents to either of these two,

$$Cr_{eq} = Cr + 1{\cdot}37Mo + 1{\cdot}5Si + 2Nb + 3Ti, \tag{8}$$

$$Ni_{eq} = Ni + 0{\cdot}31Mn + 22C + 14{\cdot}2N + Cu. \tag{9}$$

The ratio of Ni_{eq} and Cr_{eq} for any stainless steel grade determines the fraction of *d* and *g* forms during and subsequent to solidification, FP for stainless steel is expressed as (Wolf 1986)

$$FP = 5{\cdot}26\ (0{\cdot}74 - Ni_{eq}/Cr_{eq}). \tag{10}$$

The relative proportions of *d* and *g* formed during and subsequent to solidification of the different standard stainless steel grades (Ray *et al* 1997) are shown in figure 12.

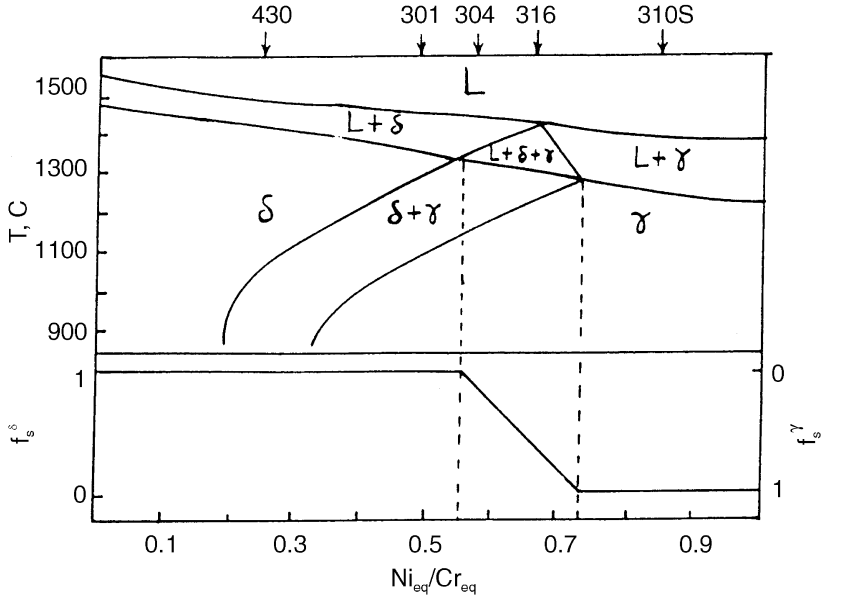

Figure 12. Relative proportions of *d* and *g* formed during and subsequent to solidification in stainless steel grades (Ray *et al* 1997).

3.2 *Microsegregation and effective shell thickness*

Microsegregation (Wolf & Kurz 1981) results in the increase of concentration of an alloying element from the original value C_o to that in the last-solidifying liquid, C_L as defined by modified Schil equation

$$C_L = C_o[1 - f_s/(ak + 1]^{k-1},$$

where k is equilibrium distribution coefficient back-diffusion parameter $a = D_s t_f$-$(l/2)^{-2}$, D_s is diffusion coefficient in solid, local solidification time $t_f = T_{LS}/(dT/dt)$, T_{LS} is temperature interval between liquidus and solidus, secondary dendrite arm spacing l is proportional to (dT/dt).

Lower values of k, D_S and T_{LS} result in high C_L and microsegregation. This in turn extensively lowers the actual solidus, T_{SA}, and increases the temperature difference between equilibrium and actual solidus $(T_{SE} - T_{SA})$.

The actual thickness, S_A, of the completely solid shell during the solidification process is proportional to $(T_{SA} - T_O)$, where T_O is the strand temperature. The temperature and the thickness corresponding to the completely solid and the mushy zone in the solidifying strand are schematically shown in figure 13. Microsegregation

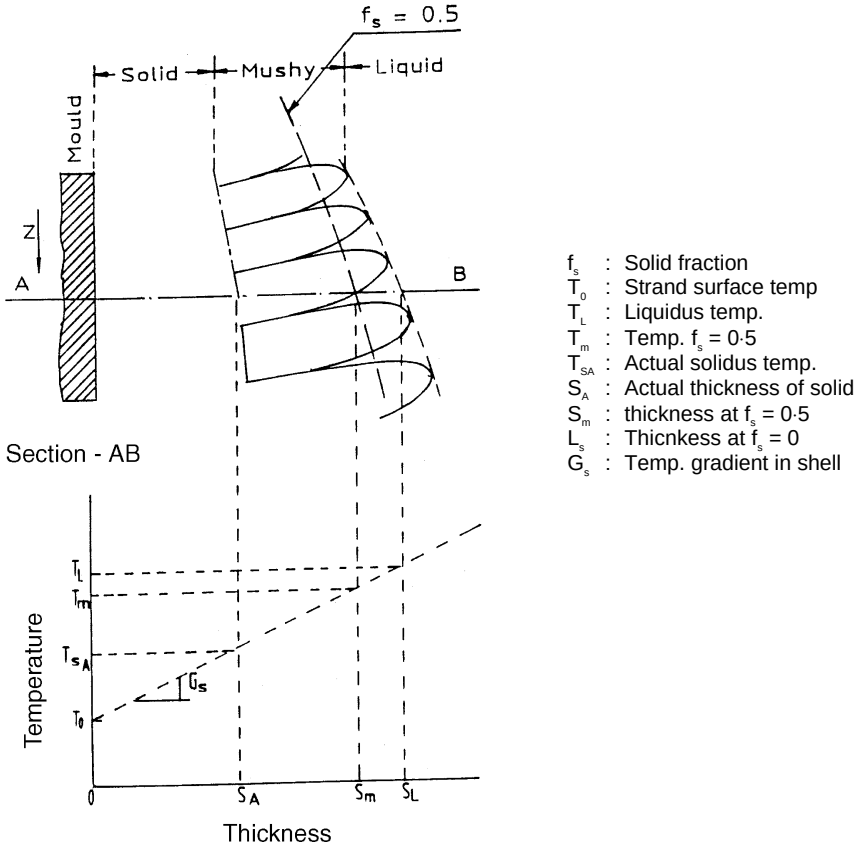

Figure 13. Temperature and thickness corresponding to solid, mushy and liquid zones.

lowers the actual solidus temperature, T_{SA}, and consequently decreases the effective thickness S_A of the solid shell.

The tramp elements, P, S and B, are very effective in causing microsegregation, when the solidification mode is predominantly *g*, because both equilibrium distribution coefficient, *k*, and diffusion coefficient D_s are low. In such eventuality the mushy zone is relatively wider, and the effective shell thickness is shallow.

3.3 *High-temperature strength and ductility*

The mushy zone in the solidification strand starts developing strength when the solid fraction exceeds 0·7 (Nakagawa *et al* 1995). The temperature corresponding to the solid fraction of 0·7, $T_{fs=0.7}$ is known as the zero strength temperature (ZST). On the other hand, the actual solidus temperature, T_{SA} i.e. the temperature at $f_s = 1{\cdot}0$, has been experimentally found to correspond to the zero ductility temperature (ZDT). These are schematically shown in figure 14, in case of solidification in the dendritic mode. (Kim *et al* 1996).

The temperature region above T_{SA} is susceptible to brittle crack formation, because the ductility is zero. However, if the cracks formed in the solidifying dendrites are accessible to the surrounding liquid, they get healed up. But when two adjacent

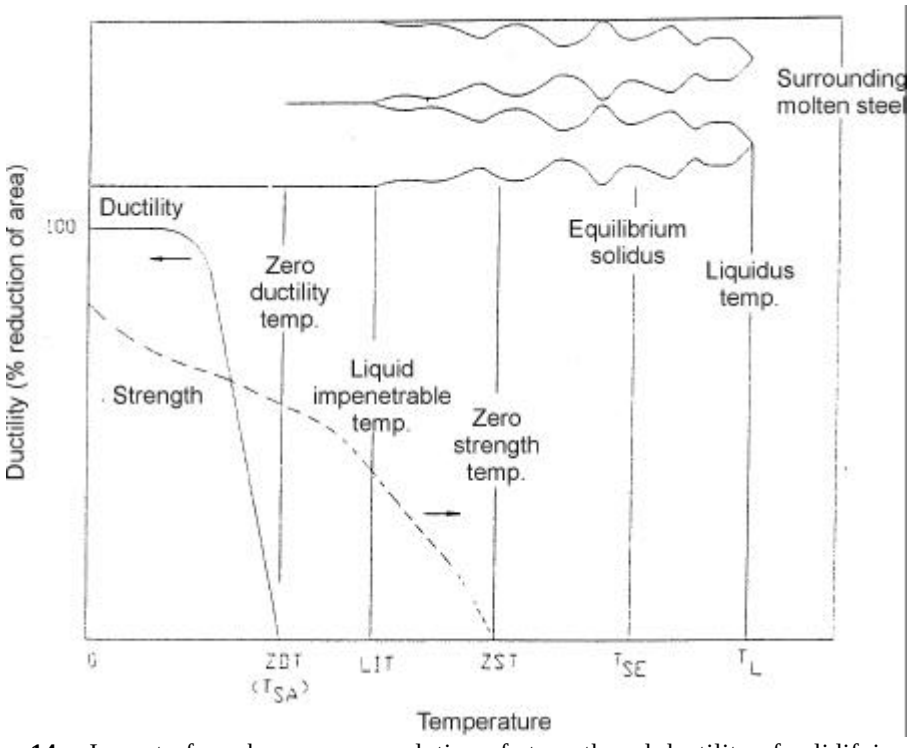

Figure 14. Impact of mushy zone on evolution of strength and ductility of solidifying shell (Kim *et al* 1996).

growing dendrites touch against each other (which has been found to correspond to the temperature at $f_s \approx 0{\cdot}9$), the surrounding liquid cannot penetrate and reach the crack site. This temperature is known as the liquid impenetrable temperature (LIT). Hence, the temperature interval (LIT – T_{SA}) corresponding to $f_s = 0{\cdot}9 \rightarrow 1$, is in reality the brittle temperature zone (Kim *et al* 1996), susceptible to formation of interdendritic, i.e. intercolumnar crack. A low-ductility temperature regime also exists between 750° and 850°C. This is usually associated with formation of intergranular crack along austenite grain boundaries. Dynamic precipitation of aluminium nitride or carbonitrides of V/Nb during deformation at low strain rate has been found to be responsible (Wolf 1991b). Coarsening of austenite grains, under hot spots associated with shell contraction or depression, enhances concentration of precipitates at the grain boundaries. This results in local embrittlement.

3.4 *Strain in brittle temperature range*

Figures 15a & b schematically show typical non-equilibrium pseudo-binary Fe–C phase diagram, and corresponding strain due to thermal contraction and $d \rightarrow g$ transformation (Kim *et al* 1996). The effect of the latter on the strain in the brittle temperature range is felt only for carbon contents between C_1 and C_2. The effect is maximum at C_{max} because the complete $d \rightarrow g$ transformation occurs in the brittle temperature range between LIT and ZDT. It is important to note that since ZDT, LIT and $d \rightarrow g$ transformation temperature are influenced by other alloying elements, C_1, C_2 and C_{max} will depend on actual steel composition.

Analysis of microsegregation and the calculation of strain in brittle temperature range are in good agreement with the frequency of longitudinal cracking (figure 16). The carbon content at which this incidence is maximum has been found to be in the range of 0·08 to 0·14%, depending on the presence of other alloying elements. In the stainless steel series the solidification behaviour of AISI 304 grade is similar to that of the 0·1% carbon grade. Incidence of surface crack and depression is likewise traced to coincidence of $d \rightarrow g$ transformation with brittle temperature range in this grade.

3.5 *Sticking vis-a-vis depression*

Tendency for mould sticking or depression formation can be traced to the relative intensity of contraction strain and bulging/bending strain. Microsegregation is minimum around 0·1% carbon, and in AISI-304 stainless grades, resulting in large effective shell thickness. The consequent large thermal contraction in this case is aided by transformation strain due to $d \rightarrow g$ transformation adjacent to the solidus. This leads to shrinking and depression formation. In contrast, complete d solidification mode for carbon contents lower than 0·05%, and for AISI-430 stainless grade, makes the shell weak due to poor creep resistance. Consequently, the bending strain owing to ferrostatic pressure forces the shell to stick to the mould. Owing to higher microsegregation for g solidification in case of higher carbon content (> 0·2%), and for AISI-310 stainless grade, the effective shell thickness is shallow, and the consequent high bending/bulging strain leads to sticking tendency.

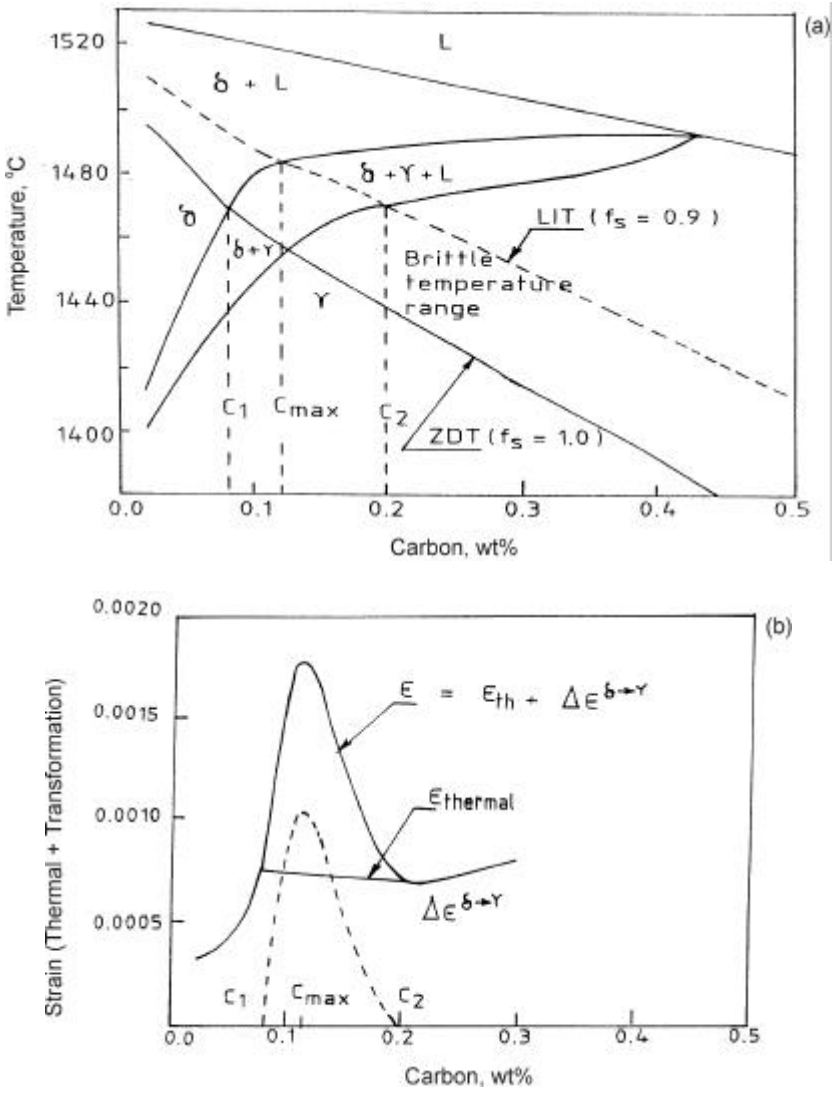

Figure 15. Effect of carbon on (**a**) brittle temperature range, and (**b**) thermal and $d \rightarrow g$ transformation strain (Kim *et al* 1996).

3.6 *Grade-specific casting parameters*

The solidification aspects elucidated above indicate the necessity of formulating the casting parameters in tune with the specific characteristics of the steel grade. The common grades can be broadly classified into three categories based on specific quality issues

- < 0·04% Carbon, high silicon, and ferritic or martensitic stainless grades have the following characteristics

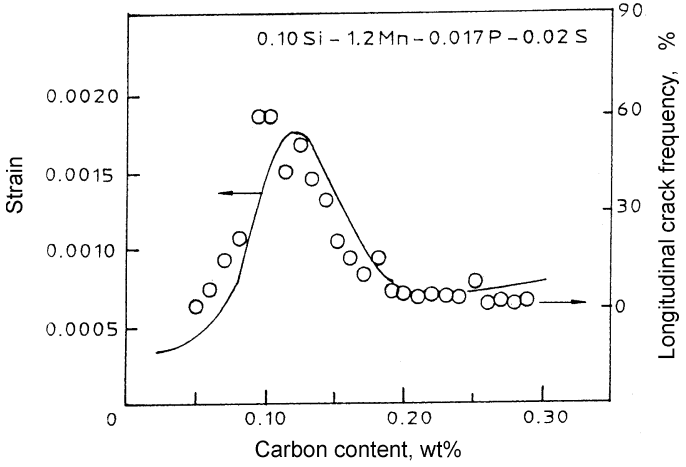

Figure 16. Correspondence of calculated strain with frequency of longitudinal crack formation (Kim *et al* 1996).

- solidification through d mode, and d is present up to 100–250°C below actual solidification temperature, T_{SA},
- the solidifying shell and the strand have very low creep strength,
- tendency for sticking in mould and bulging of strand is very high,
- cast slab in very prone to inter-columnar cracks, which may surface during subsequent rolling.

⇒ To overcome these problems mould taper has to be low (~ 0·7%), and both mould and secondary cooling intensity should be high. Basicity of mould powder should be low (< 1) to have glassy slag for better lubrication.

- 0·08% – 0·14% Carbon, and austenitic stainless (AISI-304) grades have the following characteristics

  - solidification through d mode, but $d \rightarrow g$ transformation takes place around actual solidification temperature, T_{SA},
  - the solidifying shell is thick with high creep strength,
  - high tendency for shrinkage, formation of depression along with cracks on surface and at subsurface, deep oscillation mark, and coarse grains in cast slab,
  - coarse g grains lead to embrittlement at 1000–1100°C and formation of intergranular crack in rolled product,
  - depression, subsurface crack and deep oscillation mark in cast slab leading to lamination and surface defects in rolled product.

⇒ To overcome these problems, mould taper should be high (0·9–1·0%). Mould heat transfer should be low by using powder with basicity > 1 to increase thickness of crystalline slag layer in mould.

- > = 0·25% Carbon, and AISI-310 stainless grades have following characteristics:

  – solidification predominantly through g mode with high shrinkage,
  – tendency for micro-segregation is high, resulting in deep mushy zone and thin shell,
  – tendency for strand bulging is high, resulting in inter-columnar crack, centre-line crack and macrosegregation.

⇒ Remedial measures should include large mould taper (0·9–1·0)% minimum phosphorous & sulphur, high ratio of Mn/S. High intensity of secondary cooling at the upper segments, and smaller dia rolls with low pitch are useful in minimising bulging. Central crack and macrosegregation can be minimised through low superheat, soft reduction, low casting speed, and thermal reduction.

3.7 *Chemistry optimisation*

Minor adjustment of chemistry, within the constraints of grade requirement, has proven to be a powerful tool for casting of critical grades of steel. This has been utilised to change the solidification mode, alter the relative proportion of d and g subsequent to solidification, or restrict the extent of micro-segregation.

The relative proportions of d and g during and subsequent to solidification of the stainless steels (Darle *et al* 1993) are shown in figure 2. It is evident that AISI-430 grade solidifies through d mode, and the $d \rightarrow g$ transformation starts about 300°C below the solidus for the normal chemistry. Increase in the ratio Ni_{eq}/Cr_{eq} from 0·17 to 0·22 has helped to effect earlier transformation of d to g in the strand during cooling subsequent to solidification. This has controlled coarsening of d grains and enhanced the shell strength, thereby preventing inter columnar cracking of slab (Ray *et al* 1996).

Formation of g during solidification can be avoided in AISI-304 grade by keeping the ratio Ni_{eq}/Cr_{eq} below 0·55 (Ray *et al* 1999). Decrease in this ratio from the normal level of 0.58 to 0.54, along with increase in mould taper has helped to restrict formation of longitudinal depression in concast slabs of AISI-304. This in turn has helped to considerably improve the surface quality of coils processed from these slabs.

AISI-310 solidifies entirely through g mode, and hence microsegregation is expected to be severe. Wide mushy zone along with uneven and shallow thickness of shell generates intercolumnar cracks, resulting in surface tears during hot rolling (Sen *et al* 1996). Decrease in P plus S from 0·06 to 0·04% and lowering of Ni_{eq}/Cr_{eq} from 0·9 to 0·77 have eliminated this problem.

4. Conclusions

The process of solidification during continuous casting of steel is dynamic in nature. A host of issues like heat transfer, friction/lubrication at the solid–liquid interface, high-temperature properties of solid etc. add to the complexity of the solidification process.

An integrated understanding of these factors has made the process knowledge-empowered.

Presently it is possible to control the solidification process based on the developed knowledge of the initial shell formation and mode of oscillation. This together with the grade-specific optimisation of parameters has been useful in obtaining the desirable surface as well as internal quality of cast slab.

References

Andrezejewski P, Drastik A, Kohler K U, Pluschkell W 1990 New aspects of oscillation mode operation and results in slab casting. *Process Tech. Conference Proc.* (Warrendale, PA: Iron & Steel Soc.) vol. 9, pp 173–181

Brendzy J L, Bakshi I A, Samarasekara I V, Brimacombe J K 1993 Mould-strand interaction in continuous casting of steel billets, part 2: Lubrication and oscillation mark formation. *Ironmaking Steelmaking* 20: 63–69

Brimacombe J K 1993 Intelligent mould for continuous casting of billets. *Metall. Trans*. B24: 917–928

Darle T, Mouchette A, Nadif M, Roscini M, Salvadori D 1993 Hydraulic oscillation of the CC slab mould at Soleac Florange: First industrial results, future development. *Steelmaking Conference Proc*. (Warrendale, PA: Iron & Steel Soc.) vol. 76, pp. 209–218

Harada S, Tanaka S, Misumi H 1990 A formation mechanism of transverse cracks on CC slab surface quality. South East Asian Iron & Steel Institute, pp 26–32

Hoedle H, Frauenhuber K, Moerwald K 1999 Advanced equipment for high performance casters. *Steelmaking Conference Proc*, vol. 82, pp. 141–151

Kim K, Yeo T, Oh K B, Lee D N 1996 Effect of carbon & sulphur on longitudinal surface cracks. *Iron Steel Inst. Jpn. Int.* 36: 284–292

Nakagawa T, Umeda T, Murate T 1995 Strength and ductility of solidifying shell during casting. *Trans. Iron Steel Inst. Jap.* 35: 723–728

Ray S K 2001 Effect of chemistry and solidification behaviour on quality of cast slabs and rolled products of stainless steel. *J. Mater. Performance* (accepted)

Ray S K, Mukhopadhyay B, Bhattacharyya S K 1996 Prediction of crack-sensitivity of concast slabs of AISI-430 stainless steel. *Iron Steel Inst. Jpn. Int.* 36: 611–612

Ray S K, Mukhopadhyay B, Das P C 1999 Effect of chemistry on solidification and quality of stainless steel. Presented at Annu. Tech. Mtg. of Indian Inst. Metals, Jamshedpur, 14–17 Nov. 1999

Saucedo I G 1991 Early solidification during continuous casting of steel. *Steelmaking Conference. Proc.* (Warrendale, PA: Iron & Steel Soc.) vol. 74, pp 79–89

Sen S, Mukhopadhyay B, Ray S K 1996 Continuous casting and hot rolling of AISI-310 stainless. *Steel India* 19: 18–23

Suzuki M, Mizukmi H, Kitagawa T, Kawakami K, Uchida S, Komatsu Y, 1991 Development of new mould oscillation mode for high-speed casting. *Iron Steel Inst. Jpn. Int.* 31: 254–261

Szekeres E S 1996 Overview of mould oscillation in continuous casting. *Iron Steel Eng.* July: 29–37

Tada K, Birat J P, Riboud P, Larrecq M, Hackel H 1984 Modelling of slag rim formation and pressure in molten flux near the meniscus. *Trans Iron Steel Inst. Jpn.* 24: B-382–B-387

Takeuchi E, Brimacombe J K 1984 The formation of oscillation marks in the continuous casting of steel slabs. *Metall. Trans.* B15: 493–509

Takeuchi S, Miki Y, Itoyama S, Kobayishi K, Sorimachi K, Sakuraya T 1991 Control of oscillation mark formation during continuous casting. *Steelmaking Conference Proc*. (Warrendale, PA: Iron & Steel Soc.) vol. 74, p. 303

Wolf M M 1986 Strand surface quality of stainless steel. *Ironmaking Steelmaking* 13: 248–259

Wolf M M 1991a Mould oscillation guidelines. *Steelmaking Conference Proc*. (Warrendale, PA: Iron & Steel Soc.) vol. 74, pp 51–67

Wolf M M 1991b Crack susceptibility of new grades of steel. *Proc. Ist European Conf. on Continuous* Casting, Florence, pp 2.489–2.498

Wolf M M, Kurz W 1981 Effect of carbon on solidification of steel in concast moulds. *Metall. Trans*. B12: 85–93